New Perfluoroarylborane Activators for Single-Site Olefin Polymerization. Acidity and Cocatalytic Properties of a "Superacidic" Perfluorodiboraanthracene

Matthew V. Metz, David J. Schwartz,† Charlotte L. Stern, and Tobin J. Marks*

Department of Chemistry, Northwestern University, 2145 Sheridan Road, Evanston, Illinois 60208

Peter N. Nickias

Catalysis Laboratory, The Dow Chemical Company, 1776 Building, Midland, Michigan 48674

Received January 31, 2002

The synthesis, Lewis acid properties, and single-site olefin polymerization characteristics of catalyst systems utilizing the binuclear organo-Lewis acid cocatalyst 9,10-bis(pentafluorophenyl)-9,10-diboraoctafluoroanthracene, $C_{12}F_8B_2(C_6F_5)_2$ (**8b**), are reported. X-ray diffraction analysis of **8b** reveals a nearly planar $C_{12}F_8B_2$ core with $-C_6F_5$ rings rotated 75° out of the plane, hindering π communication between the pendant $-C_6F_5$ substituents and the $C_{12}F_8B_2$ core, and thereby enhancing Lewis acidity at the boron centers. Competition equilibration experiments with **8b**, $B(C_6F_5)_3$, and acetonitrile over a wide temperature range demonstrate that **8b** is a stronger Lewis acid than $B(C_6F_5)_3$ by $\Delta H = +1.4(2)$ kcal/mol and $\Delta S = -5.3(1)$ eu. The diffraction-derived molecular structure of **8b**←$NCCH_3$ reveals substantial skeletal reorganization *only* at the coordinated boron center. When it is paired with dimethyl organo-group 4 catalyst precursors, **8b** affords extremely efficient single-site olefin polymerization systems in both laboratory and large-scale reactors. In all cases, **8b** forms polymerization systems with higher activities than those utilizing $B(C_6F_5)_3$ as the cocatalyst.

Introduction

In single-site homogeneous olefin polymerization catalysis (**1**; Figure 1),[1] organo-Lewis acids such as alumoxanes and tris(perfluoroaryl)boranes[2,3] as well as weakly coordinating perfluoroarylborates (Figures 1 and 2)[2,3a,b,d,m,4,6a] play crucial roles in catalyst activation. Furthermore, there is now convincing evidence, supported by computational studies,[5] that the nature of the catalyst−cocatalyst ion pairing, as modulated by the specific structural and electronic properties of the cocatalyst-derived counteranion (A^- in structure **1**, Figure 1),[3a−g,i−m,6] can dramatically influence polymerization activity, chain transfer rates, α-olefin enchainment regio- and stereochemistry, and catalyst stability.[3,6,7]

In this contribution we describe efforts to enhance and quantify fluoroarylborane Lewis acidity by introducing multiple communicating electron-deficient centers, a

† Current address: The Dow Chemical Co., 2301 N. Brazosport Blvd., B-1470, Freeport, TX 77541.

(1) For recent reviews see: (a) Chum, P. S.; Kruper, W. J.; Guest, M. J. *Adv. Mater.* **2000**, *12*, 1759−1767. (b) Gladysz, J. A., Ed. Frontiers in Metal-Catalyzed Polymerization (special issue). *Chem. Rev.* **2000**, *100*. (c) Marks, T. J., Stevens, J. C. Catalysts and Processes (special issue). *Adv. Polym. Catal.* **1999**, *7*, 1−208. (d) Britovsek, G. J. P.; Gibson, V. C.; Wass, D. F. *Angew. Chem., Int. Ed.* **1999**, *38*, 428−447. (e) Jordan, R. F. Ed. *J. Mol. Catal.* **1998**, *128* 1−337. (f) McKnight, A. L.; Waymouth, R. M. *Chem. Rev.* **1998**, *98*, 2587−2598. (g) Piers, W. E. *Chem. Eur. J.* **1998**, *4*, 13−18. (h) Kaminsky, W.; Arndt, M. *Adv. Polym. Sci.* **1997**, *127*, 143−187. (i) Bochmann, M. *J. Chem. Soc., Dalton Trans.* **1996**, 255−270. (j) Brintzinger, H. H.; Fischer, D.; Mülhaupt, R.; Rieger, B.; Waymouth, R. M. *Angew. Chem., Int. Ed. Engl.* **1995**, *34*, 1143−1170. (k) Marks, T. J. *Acc. Chem. Res.* **1992**, *25*, 57−65.

(2) For recent reviews on cocatalysts and related weakly coordinating anions see: (a) Pedeutour, J.-N.; Radhakrishnan, K.; Cramail, H.; Deffieux, A. *Macromol. Rapid Commun.* **2001**, *22*, 1095−1123. (b) Chen, E. Y. X.; Marks, T. J. *Chem. Rev.* **2000**, *100*, 1391−1434. (c) Piers, W. E. *Chem. Eur. J.* **1998**, *4*, 13−18. (d) Reed, C. A. *Acc. Chem. Res.* **1998**, *31*, 133−139. (e) Piers, W. E.; Chivers, T. *Chem. Soc. Rev.* **1997**, *26*, 345−354. (e) Strauss, S. H. *Chem. Rev.* **1993**, *93*, 927−942.

(3) (a) Zhou, J.; Lancaster, S. J.; Walker, D. A.; Beck, S.; Thornton-Pett, M.; Bochmann, M. *J. Am. Chem. Soc.* **2001**, *123*, 223−237. (b) Williams, V. C.; Irvine, G. J.; Piers, W. E.; Li, Z.; Collins, S.; Clegg, W.; Elsegood, M. R. J.; Marder, T. B. *Organometallics* **2000**, *19*, 1619−1621. (c) Chase, P. A.; Piers, W. E.; Patrick, B. O. *J. Am. Chem. Soc.* **2000**, *122*, 12911−12912. (d) LaPointe, R. E.; Roof, G. R.; Abboud, K. A.; Klosin, J. *J. Am. Chem. Soc.* **2000**, *122*, 9560−9561. (e) Williams, V. C.; Piers, W. E.; Clegg, W.; Elsegood, M. R. J.; Collins, S.; Marder, T. B. *J. Am. Chem. Soc.* **1999**, *121*, 3244−3245. (f) Chen, Y.-X.; Metz, M. V.; Li, L.; Stern, C. L.; Marks, T. J. *J. Am. Chem. Soc.* **1998**, *120*, 6287−6305. (g) Li, L.; Marks, T. J. *Organometallics* **1998**, *17*, 3996−4003. (h) Luo, L.; Marks, T. J. *Top. Catal.* **1999**, *7*, 97−106. (i) Deck, P. A.; Beswick, C. L.; Marks, T. J. *J. Am. Chem. Soc.* **1998**, *120*, 1772−1784. (j) Kohler, K.; Piers, W. E. *Can. J. Chem.* **1998**, *76*, 1249−1255. (k) Temme, B.; Erker, G.; Karl, J.; Luftmann, H.; Frohlich, R.; Kotila, S. *Angew. Chem., Int. Ed. Engl.* **1995**, *34*, 1755−1757. (l) Yang, X.; Stern, C. L.; Marks, T. J. *J. Am. Chem. Soc.* **1994**, *116*, 10015−10031. (m) Jia, L.; Yang, X.; Stern, C. L.; Marks, T. J. *Organometallics* **1994**, *13*, 3755−3757.

(4) (a) Chien, J. C. W.; Tsai, W. M.; Rausch, M. D. *J. Am. Chem. Soc.* **1991**, *113*, 8570−8571. (b) Ewen, J. A.; Elder, M. J. Preparation of Metallocene Catalysts for Polymerization of Olefins (Fina Technology, Inc.). Eur. Patent EP0426637, May 8, 1991. (c) Hlatky, G. G.; Upton, D. J.; Turner, H. W. Supported Ionic Metallocene Catalysts for Olefin Polymerization (Exxon Chemical Patents, Inc.). WO 9109882, July 7, 1991. (d) Turner, H. W. Soluble Catalysts for Polymerization of Olefins (Exxon Chemical Patents, Inc., USA) Eur. Patent EP 277004A1, Aug 3, 1988. (e) Yang, X.; Stern, C.; Marks, T. J. *Organometallics* **1991**, *10*, 840−842.

10.1021/om020079b CCC: $22.00
Publication on Web 08/24/2002

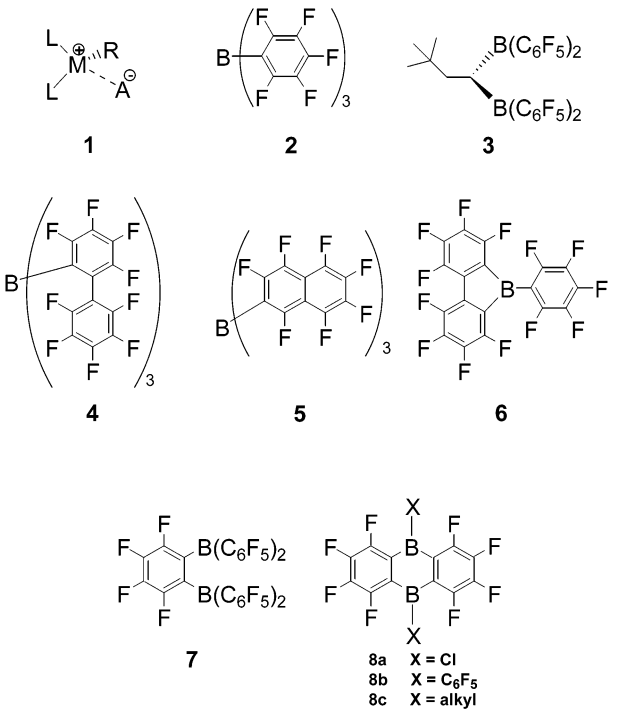

Figure 1. Active single-site polymerization catalyst (**1**) and representative perfluoroarylborane cocatalysts.

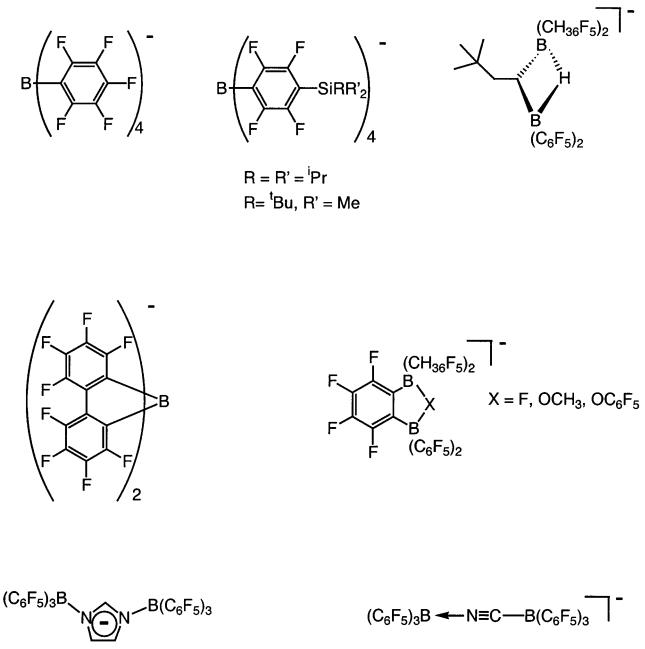

Figure 2. Representative perfluoroarylborate counteranion structures used in single-site olefin polymerization catalysis.

sterically open structure, and conjugative delocalization of negative charge. To achieve this, we selected the perfluorodiboraanthracene skeleton **8** (Figure 1; see ref 8 for earlier nonfluorinated analogues), where computation at the B3LYP/6-31++G** level indicates that **8b** has ~10 kcal/mol greater CH_3^- affinity than does $B(C_6F_5)_3$.[9] An important structural aspect of single-site olefin polymerization is the facility with which some transition-metal catalyst systems, such as those having "constrained geometries,"[1a,10] exhibit high polymerization activities while enchaining unusually high levels of sterically encumbered α-olefin comonomers and long-chain branches into the polymer backbone. For this reason, constrained-geometry catalysts were of particular interest in this study.

The present contribution provides a full discussion of the structure, Lewis acid properties, and cocatalytic characteristics of perfluoroaryldiborane **8b**.[11] We report that the octafluorodiboraanthracene molecular core of **8b** provides an expansive, electron-deficient framework with which to delocalize negative charge, generating the most Lewis acidic perfluoroarylborane prepared to date. It will be seen that the molecular core forces the pendant $-C_6F_5$ substituents to twist out of the $C_{12}F_8B_2$ plane, which hinders π electron donation to the diboraanthracene core and contributes to the high Lewis acidity, which is thermodynamically quantified here in competition experiments. The combination of high Lewis acidity and weak coordinating tendency leads to highly efficient **8b**-based single-site catalytic polymerization systems. The olefin polymerization characteristics of **8b** have been examined with a range of group 4 dimethyl complexes in both benchtop and large-scale reactors. Large-scale batch polymerizations show catalyst systems derived from **8b** to be extremely active (1.5×10^8 g of polymer/((mol of catalyst)(atm of monomer) h) and long-lived (≥15 min at 140 °C) for the polymerization of propylene and the copolymerization of ethylene and 1-octene.

(5) (a) Lanza, G.; Fragalà, I. L.; Marks, T. J. *Organometallics* **2001**, *20*, 4006−4017. (b) Vanka, K.; Ziegler, T. *Organometallics* **2001**, *20*, 905−913. (c) Lanza, G.; Fragalà, I. L.; Marks, T. J. *J. Am. Chem. Soc.* **2000**, *122*, 12764−12777. (d) Chan, M. S. W.; Ziegler, T. *Organometallics* **2000**, *19*, 5182−5189. (e) Rappé, A. K.; Skiff, W. M.; Casewit, C. J. *Chem. Rev.* **2000**, *100*, 1435−1456. (f) Vanka, K.; Chan, M. S. W.; Pye, C.; Ziegler, T. *Organometallics* **2000**, *19*, 1841−1849. (g) Chan, M. S. W.; Vanka, K.; Pye, C. C.; Ziegler, T. *Organometallics* **1999**, *18*, 4624−4636. (h) Lanza, G.; Fragalà, I. L. *Top. Catal.* **1999**, *15*, 45−60. (i) Lanza, G.; Fragalà, I. L.; Marks, T. J. *J. Am. Chem. Soc.* **1998**, *120*, 8257−8258. (j) Fusco, R.; Longo, L.; Proto, A.; Masi; F.; Garbasi, F. *Macromol. Rapid Commun.* **1998**, *19*, 257−262. (k) Fusco, R.; Longo, L.; Masi, F.; Garbasi, F. *Macromolecules* **1997**, *30*, 7673−7685. (l) Fusco, R.; Longo, L.; Masi, F.; Garbasi, F. *Macromol. Rapid Commun.* **1997**, *18*, 433−441.

(6) (a) Jia, L.; Yang, X.; Stern, C. L.; Marks, T. J. *Organometallics* **1997**, *16*, 842−857. (b) Giardello, M. A.; Eisen, M. S.; Stern, C. L.; Marks, T. J. *J. Am. Chem. Soc.* **1995**, *117*, 12114−12129.

(7) (a) Chen, M.-C.; Marks, T. J. *J. Am. Chem. Soc.* **2001**, *123*, 11803−11804. (b) Shiomura, T.; Uchikawa, N.; Asanuma, T.; Sugimoto, R.; Fujio, I.; Kimura, S.; Harima, S.; Akiyama, M.; Kohno, M.; Inoue, N. In *Metallocene-Based Polyolefins*; Scheirs, J., Kaminsky, W., Eds.; Wiley: Chichester, U.K., 2000; pp 437−465. (c) Shiomura, T.; Asanuma, T.; Inoue, N. *Macromol. Rapid Commun.* **1996**, *17*, 9−14. (d) Siedle, A. R.; Hanggi, B.; Newmark, R. A.; Mann, K. R.; Wilson, T. *Macromol. Symp.* **1995**, *89*, 299−305.

(8) (a) Mueller, P.; Huck, S.; Koeppel, H.; Pritzkow, H.; Siebert, W. *Z. Naturforsch., B: Chem. Sci.* **1995**, *50*, 1476−1484. (b) Schulz, H.; Pritzkow, H.; Siebert, W. *Chem. Ber.* **1991**, *124*, 2203−2207

(9) McAdon, M. H. Dow Chemical Co., personal communication.

(10) (a) Li, L.; Li, H.; Metz, M. V.; Chen, M.-C.; Rheingold, A. L.; Liable-Sands, L. M.; Marks, T. J. *J. Am. Chem. Soc.*, in press. (b) Marks, T. J.; Li, L.; Metz, M. V.; Rheingold, A. L.; Liable-Sands, L. M. *Abstr. Pap.-Am. Chem. Soc.* **2001**, *221*, INOR-569. (c) Li, L.; Metz, M. V.; Marks, T. J.; Liable-Sands, L.; Rheingold, A. L. *Polym. Prepr. (Am. Chem. Soc., Div. Polym. Chem.)* **2000**, *41*, 1912−1913. (d) Li, L.; Marks, T. J.; Liable-Sands, L. M.; Rheingold, A. L.; Metz, M. V. *Abstr. Pap.-Am. Chem. Soc.* **2000**, *220*, POLY-406.

(11) (a) Metz, M. V.; Schwartz, D. J.; Stern, C. L.; Nickias, P. N.; Marks, T. J. *Angew. Chem., Int. Ed.* **2000**, *39*, 1312−1316. (b) McAdon, M. H.; Nickias, P. N.; Marks, T. J.; Schwartz, D. J. Activators for Transition Metal Complex Catalysts for Polymerization of Olefins (The Dow Chemical Co.; Northwestern University). WO-A 9906413A1, Feb 11, 1999. (c) See ref 17 in: Williams, V. C.; Piers, W. E.; Clegg, W.; Elsegood, M. R. J.; Collins, S.; Marder, T. *J. Am. Chem. Soc.* **1999**, *121*, 3244−3245.

Experimental Section

Materials and Methods. Manipulations of air-sensitive materials were carried out with rigorous exclusion of oxygen and moisture in flamed Schlenk-type glassware on a dual-manifold Schlenk line or interfaced to a high-vacuum line (10^{-6} Torr), or in a nitrogen-filled glovebox with a high-capacity recirculator (<1 ppm of O_2). Argon, ethylene, and propylene (Matheson, polymerization grade) were purified by passage through supported MnO oxygen removal and activated Davison 4A molecular sieve columns. Ether solvents were purified by distillation from Na/K alloy/benzophenone ketyl, and hydrocarbon solvents were distilled from Na/K alloy. All solvents for high-vacuum-line manipulations were stored in vacuo over Na/K alloy in Teflon-valved bulbs. Deuterated solvents obtained from Cambridge Isotope Laboratories (all >99 atom % D) were freeze−pump−thaw degassed, dried over Na/K alloy, and stored in resealable flasks. Other nonhalogenated solvents were dried over Na/K alloy, while halogenated solvents were distilled from P_2O_5 and stored over activated Davison 4A molecular sieves. CH_3CN (Aldrich) was dried over CaH_2 and then over activated 4A molecular sieves before vacuum transfer. The precatalysts Cp_2ZrMe_2,[11] CGCTiMe_2,[12] $Me_2Si(Ind)_2ZrMe_2$,[13] and $(C_5Me_5)_2ZrMe_2$[14] were prepared by published procedures.

Physical and Analytical Measurements. NMR spectra were recorded on Varian VXR 300 (FT 300 MHz, ^{1}H; 75 MHz, ^{13}C), Unity 400 (FT 400 MHz, ^{1}H; 100 MHz, ^{13}C; 377 MHz, ^{19}F), or Gemini-300 (FT 300 MHz, ^{1}H; 75 MHz, ^{13}C; 282 MHz, ^{19}F) instruments. Chemical shifts for ^{1}H and ^{13}C spectra were referenced using internal solvent resonances and are reported relative to tetramethylsilane. ^{19}F NMR spectra were referenced to external $CFCl_3$. NMR experiments on air-sensitive samples were conducted in Teflon valve sealed sample tubes (J. Young). Melting temperatures of polymers were measured by DSC (DSC 2920, TA Instruments, Inc.) from the second scan with a heating rate of 10 °C/min.

Synthesis of $C_{12}F_8B_2Cl_2$ (8a). On the vacuum line, excess BCl_3 (5.0 g, 44 mmol) was condensed at −196 °C into a thick-walled reaction tube fitted with a J. Young valve and containing 5.3 g (11.1 mmol) of 1,2-$C_6F_4(SnMe_3)_2$.[18] The flask was then evacuated to 0.05 Torr, the valve was closed, and the reaction mixture was heated at 180 °C for 18 h. (*Caution*! In addition to evacuating the system prior to heating, the reaction tube should be enclosed in a steel pipe behind a blast shield.) After the reaction mixture was cooled to 25 °C, excess BCl_3 was removed under dynamic vacuum, yielding a beige, slightly moist crude product. The crude product was extracted with pentane (3 × 20 mL), leaving behind after filtration ca. 65% of the Me_3SnCl reaction product. The remaining Me_3SnCl was removed by vacuum sublimation at 40 °C/10^{-5} Torr. The desired diboraanthracene product was then collected by sublimation at 90 °C/10^{-5} Torr, affording **8a** as a yellow polycrystalline solid (1.15 g, 53% yield). ^{19}F NMR (C_6D_6): δ −122.7 (m, 4F), −143.9 (m, 4F) ppm. ^{13}C NMR ($CDCl_3$): δ 152.6 (d, $^1J_{CF}$ = 262 Hz), 144.6 (d, $^1J_{CF}$ = 260 Hz), 122.8 (br, B−C) ppm. MS (EI, 8.7 V; *m*/*z* (% intensity)): 392 (16), 391 (18), 390 (67), 389 (M^+, 47), 388 (100), 387 (51), 342 (21), 318 (22), 304 (28), 250 (25), 201 (30). Anal. Calcd for $C_{12}F_8B_2Cl_2$: C, 37.1; H, 0.0. Found: C, 38.2; H, 0.3.

Synthesis of $C_{12}F_8B_2(C_6F_5)_2$ (8b). A thick-walled tube fitted with a J. Young valve was charged with 0.265 g of **8a** (0.68 mmol) and 0.33 g of $(C_6F_5)_2SnMe_2$[15] (0.68 mmol). The flask was then attached to the vacuum line and cooled to −78 °C, 20 mL of toluene was condensed in, and the valve was closed. The reaction solution was next heated to 140 °C for 72 h, affording a bright yellow solution. After the mixture was cooled to room temperature, the solvent was removed by bulb-to-bulb distillation under dynamic vacuum. The Me_2SnCl_2 reaction product was also removed under dynamic vacuum (10^{-5} Torr/12 h). The crude **8b** was then recrystallized twice from 10 mL of toluene (slow cooling to −78 °C), giving the desired product as a light yellow crystalline solid (0.35 g, 80% yield). ^{19}F NMR (toluene-d_8): δ −118.2 (br, 4F, ortho C_6F_4), −133.9 (dd, $^3J_{FF}$ = 25.1 Hz; $^4J_{FF}$ = 7.9 Hz, 4F, ortho C_6F_5), −138.9 (m, 4F, meta C_6F_4), −152.1 (t, $^3J_{FF}$ = 21 Hz, 2F, para C_6F_5), −161.4 (ddd, $^3J_{FF}$ = 22 Hz; $^3J_{FF}$ = 22 Hz, $^5J_{FF}$ = 7 Hz, 4F, meta C_6F_5) ppm. ^{13}C NMR ($CDCl_3$): δ 156.1 (d, $^1J_{CF}$ = 267 Hz), 145.9 (d, $^1J_{CF}$ = 265 Hz), 144.3 (d, $^1J_{CF}$ = 241 Hz), 141.6 (d, $^1J_{CF}$ = 265 Hz), 137.6 (d, $^1J_{CF}$ = 253 Hz), 128.3 (br), 123.7 (br) ppm. Anal. Calcd for $C_{24}F_{18}B_2$: C, 44.22; H, 0.00. Found: C, 42.61; H, 0.52. This compound proved difficult to combust, resulting in consistently low C analyses, despite attempts with X-ray-quality crystals.

Equilibration of Acetonitrile between $B(C_6F_5)_3$ and 8b. A J. Young NMR tube was charged with **8b** (0.0100 g, 0.015 mmol) and $CH_3CN{\rightarrow}B(C_6F_5)_3$[3g] (0.0085 g, 0.015 mmol) in the glovebox, and C_7D_8 was added. The temperature of the NMR spectrometer was set to the desired temperature and the temperature confirmed by the line separation of ethylene glycol or methanol temperature calibration standards. The **8b** + CH_3CN + $B(C_6F_5)_3$ solution was placed into the spectrometer and allowed to equilibrate for 1.0 h, and the spectrum was then recorded. This procedure was repeated until spectra had been obtained at 40, 30, 21, 0, −10, −22, −27, and −47 °C. Integration of the *para* fluorine signals on $B(C_6F_5)_3$ and $CH_3CN{\rightarrow}B(C_6F_5)_3$ was used to determine the equilibrium concentrations. At no time during the equilibrations, at any temperature, were any peaks assignable to a bis(acetonitrile) adduct of **8b** detected. All peaks in the spectra can be readily assigned to resonances of $B(C_6F_5)_3$, $CH_3CN{\rightarrow}B(C_6F_5)_3$, **8b**, or **8b**←$NCCH_3$.

Synthesis of $C_{12}F_8B_2(C_6F_5)_2$←$NCCH_3$, (8b←$NCCH_3$). A J. Young NMR tube was charged with **8b** (0.0100 g, 0.015 mmol) and $CH_3CN{\rightarrow}B(C_6F_5)_3$[3g] (0.0085 g, 0.015 mmol) in the glovebox, and C_7D_8 was added. The mixture was allowed to stand at room temperature for 1 week, affording colorless needles of $CH_3CN{\rightarrow}$**8b** (0.0071 g, 67% yield). ^{19}F NMR (toluene-d_8): δ −122.5 (d, 2 F, $^3J_{FF}$ = 18 Hz), −132.9 (d, 2 F, $^3J_{FF}$ = 18 Hz), −134 (br, 2 F), −136.4 (d, 2 F, $^3J_{FF}$ = 23 Hz), −144.2 (dd, 2 F, $^3J_{FF}$ = 29 Hz, $^4J_{FF}$ = 13 Hz), −154.3 (t, 1 F, $^3J_{FF}$ = 20 Hz), −154.9 (d, 2F, $^3J_{FF}$ = 20 Hz), −156.4 (t, 1 F, $^3J_{FF}$ = 21 Hz), −162 (br, 2 F), −163.0 (dd, 2 F, $^3J_{FF}$ = 21, $^4J_{FF}$ = 8 Hz). ^{1}H NMR (toluene-d_8): δ 2.18 (s, 3 H). Anal. Calcd for $C_{26}H_3B_2NF_{18}$: C, 45.07; H, 0.44; N, 2.02. Found: C, 44.86; H, 0.53; N, 1.94.

In Situ Generation and Spectroscopy of Ion Pair 10. In the glovebox, **8b** (0.0051 g, 8.0 μmol) and Cp_2ZrMe_2 (0.0020 g, 8.0 μmol) were charged into a J. Young NMR tube. The tube was removed from the glovebox and interfaced to the high-vacuum line, and CD_2Cl_2 was condensed in at −78 °C. The solution was maintained at −78 °C until introduction into the spectrometer probe. ^{19}F NMR (CD_2Cl_2, 25 °C): δ −123.1 (br,

(12) Samuel, E.; Rausch, M. D. *J. Am. Chem. Soc.* **1973**, *95*, 6263−6267.

(13) (a) Stevens, J. C.; Timmers, F. J.; Wilson, D. R.; Schmidt, G. F.; Nickias, P. N.; Rosen, R. K.; Knight, G. W.; Lai, S. Y. Constrained Geometry Addition Polymerization Catalysts, Processes for Their Preparation, Precursors Therefor, Methods of Use, and Novel Polymers Formed Therewith; (Dow Chemical Co.). Eur. Patent EP0416815, March 13, 1991. (b) Canich, J. M.; Hlatky, G. G.; Turner, H. W. Aluminum-Free Monocyclopentadienylmetallocene Catalysts for Olefin Polymerization; (Exxon Chemical Patents, Inc.). WO-9200333 A2, Jan 9, 1992. (c) Canich, J. A. M. Olefin Polymerization Catalysts (Exxon Chemical Patents, Inc.). Eur. Patent EP-420436A1, April 3, 1991.

(14) (a) Herrmann, W. A.; Herdtweck, E.; Winter, A.; Spaleck, W.; Rohrmann, J. *Angew. Chem., Int. Ed. Engl.* **1989**, *28*, 1511−1512. (b) Herfert, N.; Fink, G. *Makromol. Chem., Rapid Commun.* **1993**, *14*, 91−96.

(15) Manriquez, J. M.; McAlister, D. R.; Sanner, R. D.; Bercaw, J. E. *J. Am. Chem. Soc.* **1978**, *100*, 2716−2724.

(16) Fenton, D. E.; Massey, A. G.; Jolley, K. W.; Sutcliffe, L. H. *Chem. Commun.* **1967**, 1097−1098.

(17) Sheldrick, G. M. SHELXS-97; University of Göttingen, Göttingen, Germany, 1990.

(18) Sheldrick, G. M. SHELXL-97; University of Göttingen, Göttingen, Germany, 1997.

2F, F7; see Figure 9 for assignments), −132.4 (m, 3F, F3 + F4 or F8), −134.0 (br, 2F, F4 or F8), −134.8 (br, 1F, F3), −145.0 (br, 2F, F6), −155.4 (t, $^3J_{FF}$ = 21 Hz, 1F, F10), −158.9 (m, 2F, F5), −160.0 (m, 1F, F1), −161.8 (br, 1F, F2), −162.5 (br, 1F, F2), −164.1 (br, t, 3JFF = 21 Hz, 2F, F9) ppm. ^{1}H NMR (CD_2Cl_2, 25 °C): δ 6.34 (s, 10H), 0.66 (s, 3H), 0.17 (br, 3H) ppm.

In Situ Generation and Spectroscopy of Ion Pair 11. In the glovebox, **8b** (0.0051 g, 8.0 μmol) and Cp_2ZrMe_2 (0.0040 g, 16.0μmol) were charged into a J. Young NMR tube. The tube was removed from the glovebox, interfaced to the high-vacuum line, and CD_2Cl_2 was condensed in at −78 °C. The solution was maintained at −78 °C until introduced into the spectrometer probe. ^{19}F NMR (CD_2Cl_2, 25 °C): δ − 132.7 (br, 2F, ortho C_6F_5), −134.7 (br, 4F, ortho C_6F_4), −136.4 (br, 2F, ortho C_6F_5), −161.6 (t, $^3J_{FF}$ = 20 Hz, 2F, para C_6F_5), −162.6 (d, $^3J_{FF}$ = 19 Hz, 4F, meta C_6F_4), −164.4 (br, 2F, meta C_6F_5), −165.4 (br, 2F, meta C_6F_5) ppm. ^{1}H NMR (CD_2Cl_2, 25 °C): δ 6.22 (s, 10H), 0.69 (s, 3H), 0.19 (br, 3H) ppm; a slight excess of $(C_5H_5)_2ZrMe_2$ was present in this sample, and resonances attributable to this compound are also detected.

Procedure for Single-Crystal Structural Characterization. In the glovebox, crystals were placed on a glass slide and covered with dry Infineum V8512 (formerly Paratone-N) oil. The crystals were then removed from the box, and a suitable crystal was chosen under a microscope using plane-polarized light. The crystal was mounted on a glass fiber and transferred to the cold stage of a Bruker SMART 1000 CCD area detector in a nitrogen cold stream at 153(2) K. Twenty frames (usually 20 exposures, 0.3° slices) were collected in three areas of reciprocal space to determine the orientation matrix. The parameters for data collection were determined by the peak intensities and widths from the 60 frames used to determine the orientation matrix. The faces of the crystal were then indexed and data collection initiated. After data collection, the frames were integrated, the initial crystal structure was solved by direct methods, the structure solution was expanded through successive least-squares cycles, absorption corrections were applied, and the final solution was determined. SHELXS-97[16] was used for the initial solution, and SHELXL-97[17] was used to refine the structure.

Laboratory-Scale Polymerization Experiments. This procedure is designed to minimize mass transfer (gas to solution; catalyst entrainment) and exotherm effects while at the same time maintaining strictly anaerobic/anhydrous conditions.[3f] On a high-vacuum line (10^{-6} Torr), ethylene and propylene polymerizations were carried out in a 250 mL round-bottom three-neck Morton flask equipped with a large magnetic stirring bar and a thermocouple probe. In a typical experiment, a measured quantity of dry toluene, 100 mL for ethylene and 50 mL for propylene polymerizations, was vacuum-transferred into the flask, presaturated under 1.0 atm of rigorously purified ethylene or propylene (pressure maintained at 1.0 atm using a mercury bubbler), and equilibrated at the desired reaction temperature using an external bath. The catalytically active species was then freshly generated (within 5.0 min) using a solution having either a 1:1 (Table 4, entries 1−4 and 6−12) or 2:1 (Table 4, entry 5) metallocene to cocatalyst ratio in ~2 mL of dry 1,2-$C_6H_4F_2$. The catalyst solution was then quickly injected into the rapidly stirred flask using a gastight syringe equipped with a flattened spraying needle. The temperature of the toluene solution in representative polymerization experiments was continuously monitored using a thermocouple (OMEGA Type K thermocouple with a model HH21 microprocessor thermometer). After a measured time interval (short to minimize mass transport and exotherm effects), the polymerization was quenched by the addition of 20 mL of 2% acidified methanol. Another 30 mL of methanol was then added, and the polymer was collected by filtration, washed with methanol, and dried under vacuum overnight to a constant weight. Activities given in Table 4 are the average of two trials; the reproducibility was within ±10%.

Large-Scale Polymerization Experiments. All large-scale polymerizations were performed at the Dow Chemical Co. Polyolefins Catalysis Laboratory. Entries 9 and 10 were carried out in a stirred 2.0 L Parr reactor charged with 740 g of Isopar-E mixed alkanes solvent and 118 g of 1-octene comonomer.[3g] Hydrogen was added to control polymer molecular weight by differential pressure expansion from a 75 mL addition tank at 25 psi. The reactor was heated to 140 °C and saturated with ethylene at 500 psig. Then 2.0 μmol each of catalyst and cocatalyst (0.005 M in toluene) were premixed in the glovebox; the solution was transferred to a catalyst addition tank and injected into the reactor. Polymerization conditions were maintained for 15 min with ethylene on demand. The resulting polymer solutions were removed from the reactor, and a phenol antioxidant (Irganox 1010) was added. Polymers were recovered by removal of solvent in vacuo at 120 °C for 20 h. Entries 11 and 12 were carried out in a stirred 2.0 L autoclave reactor charged with 640 g of Isopar-E mixed alkanes solvent and 216 g of propylene. Hydrogen (26 psi) was added to control polymer molecular weight. The reactor was heated to 70 °C, and a 0.0050 M catalyst/cocatalyst solution in toluene was injected into the reactor with rapid stirring. Polymerization conditions were maintained for 10 min.

Results and Discussion

The dichlorodiboraanthrancene precursor to **8b**, **8a**, was prepared via reaction of the known ditin reagent 1,2-$C_6F_4(SnMe_3)_2$[18] with BCl_3 at high temperature (Scheme 1). As judged by ^{19}F NMR, monosubstituted 1,2-$C_6F_4(SnMe_3)BCl_2$ (**9**) is formed initially, with subsequent heating affording **8a** in high yield. There is no NMR evidence for 1,2-$C_6F_4(BCl_2)_2$ at any time during the course of the conversion. This result stands in contrast to nonfluorinated 1,2-$C_6H_4(SnMe_3)_2$, which undergoes rapid B−Sn metathesis with BCl_3 at 25 °C to yield 1,2-$C_6H_4(BCl_2)_2$[19] (eq 1). Similarly, both 1,2-

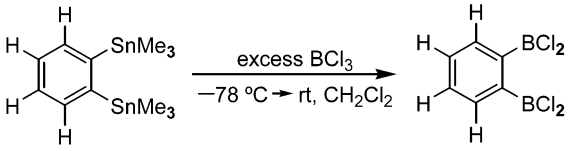

(1)

$C_6H_4(SiMe_3)BCl_2$ and 1,2-$C_6H_4(BCl_2)_2$ are readily formed from 1,2-$C_6H_4(SiMe_3)_2$ and BCl_3 under mild conditions (eq 2).[20] It is reasonable to hypothesize that the de-

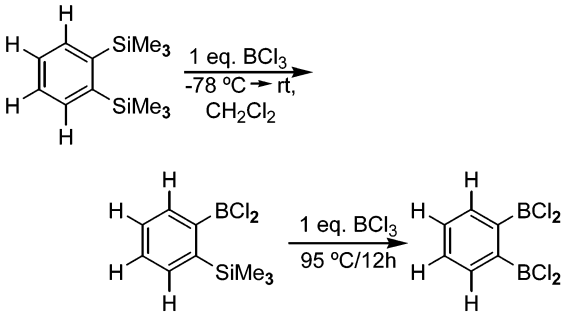

(2)

creased nucleophilicity of the fluorinated dimetalloid disfavors the second electrophilic aromatic substitution/

(19) Chivers, T. *J. Organomet. Chem.* **1969**, *19*, 75−80.
(20) Kaufmann, D. *Chem. Ber.* **1987**, *120*, 901−905.

Scheme 1. Synthesis of Diboraanthracene 8b

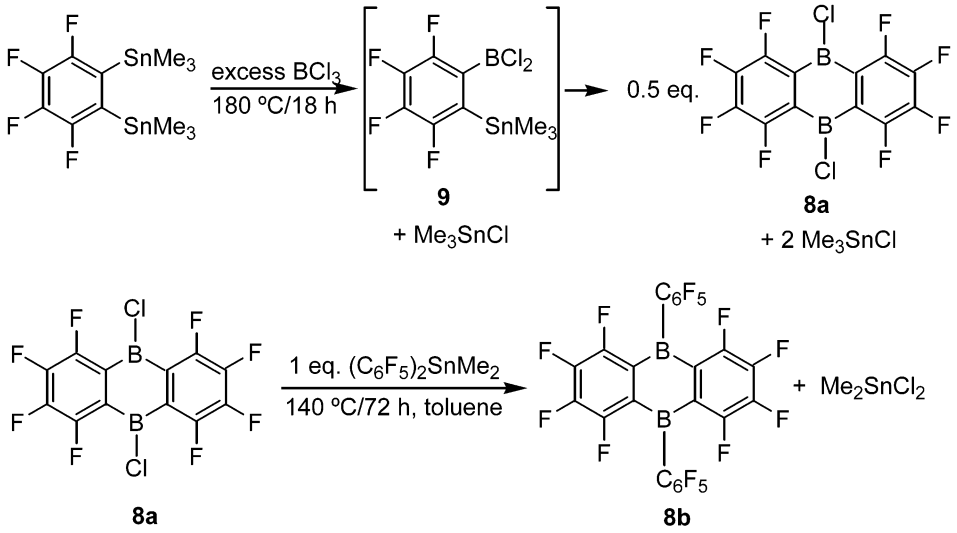

metalloid metathesis process versus coupling to yield a diboraanthracene.

Synthesis of the New Cocatalyst 1,2,3,4,5,6,7,8-Octafluoro-9,10-bis(pentafluorophenyl)-9,10-dihydro-9,10-diboraanthracene, $C_{12}F_8B_2(C_6F_5)_2$ (8b). Reaction of dichlorodiboraanthrancene **8a** with 1.0 equiv of $(C_6F_5)_2SnMe_2$ at high temperature yields $C_{12}F_8B_2(C_6F_5)_2$ (**8b**) as a pale yellow, air-sensitive crystalline solid (Scheme 1). Although this conversion requires prolonged heating, it is essentially quantitative, and the crude reaction mixture contains the final product in ≥95% purity. For selective B−Cl → B−C_6F_5 exchange, $(C_6F_5)_2SnMe_2$[21] serves as a mild reagent, effecting little or no competing alkyl group exchange.[22] In contrast, attempts to arylate **8a** with LiC_6F_5 in either pentane or ether afford a complex mixture of products, while reaction with $C_6F_5SnR_3$ (R = Me, ^{n}Bu) results in clean chloride → alkyl conversion, yielding the corresponding $C_6F_5SnR_{3-x}Cl_x$ products and, as assessed by NMR, dialkyldiboraanthracene **8c**.

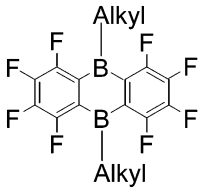

8c

Diboraanthracene **8b** was characterized by conventional spectroscopic and analytical techniques (see Experimental Section for data) and by X-ray diffraction. The ^{19}F NMR reveals significant *upfield* displacements of the C_6F_5 ortho, meta, and para signals vs $B(C_6F_5)_3$ (−5, −2, and −10 ppm, respectively, versus $B(C_6F_5)_3$), while the C_6F_4 signals are shifted considerably *downfield* of those in the dichloro species **8a** (+5, +5 ppm) and in $B(C_6F_5)_3$. The ^{19}F resonances of the C_6F_5 substituents are displaced in the opposite direction of the ^{19}F signals in the $C_{12}F_8B_2$ core. These data argue for minimal π conjugative interaction of the C_6F_5 rings in **8b** with the $C_{12}B_2F_8$ π system, which is undoubtedly electron-deficient. If the two π systems were in greater electronic communication, there should qualitatively be less dispersion in the ^{19}F resonances or, at the least, displacements in the same direction.

Table 1. Crystal Structure Data for Complexes 8b and 8b-NCCH$_3$.

	8b	**8b**-NCCH$_3$
formula	$C_{24}B_2F_{18}\cdot 2C_7H_8$	$C_{26}H_3B_2F_{18}N$
fw	836.13	692.91
cryst color, habit	yellow, rectangular	colorless, needle
cryst dimens (mm)	0.48 × 0.38 × 0.27	0.28 × 0.06 × 0.05
cryst syst	monoclinic	monoclinic
a, Å	22.8549(15)	15.0421(12)
b, Å	10.8649(7)	11.9524(10)
c, Å	13.7497(9)	13.7903(11)
α, deg	90.00	90.00
β, deg	99.6890(10)	91.832(2)
γ, deg	90.00	90.00
V, Å^3	3365.6(4)	2478.1(3)
space group	*P*2$_1$/*c* (No. 14)	*P*2$_1$/*c* (No. 14)
Z	4	4
d(calcd), g/cm^3	1.650	1.857
μ, mm^{-1}	0.165	0.203
2*θ* range, deg	1.81−28.27	1.35−28.29
no. of intensities (unique, R_i)	30 061 (8069, 0.0498)	15 453 (5809, 0.0687)
transmission factors	0.9309−0.9611	0.9587−0.9897
no. of intensities >2.0*σ*	8069	5809
abs cor	face centered, SADABS	
no. of params	523	436
final *R* indices (*I* > 2*σ*)		
R1	0.0424	0.0419
wR2	0.1183	0.0754
largest peak, hole in diff map (e/Å^3)	0.352, −0.235	0.254, −0.235

Solid-State Molecular Structure of $C_{12}F_8B_2(C_6F_5)_2$ (8b). Crystallographic parameters for **8b** are given in Table 1 and selected bond distances and bond angles in Table 2. In the structure of **8b** (Figure 3), the $C_{12}B_2F_8$ skeleton is planar, with an average atomic deviation from the mean plane of 0.013(2) Å. The C_6F_4 fragments are bent slightly out of the central B_2C_4 plane, with an average inter-ring dihedral angle of 0.6(2)°. The C_6F_5 rings are twisted out of the diboraanthracene plane, no doubt for steric reasons, with the crystallographically independent $(C_6F_4B)_2/C_6F_5$ twist angles both being 75°. In the related borafluorene **6**[3c] (Figure 1), the pentafluorophenyl ring is rotated 53.2(1)° from the $C_{12}F_8B$ plane,

(21) Schacht, W.; Kaufmann, D. *J. Organomet. Chem.* **1987**, *331*, 139−152.
(22) Chambers, R. D.; Chivers, T. *J. Chem. Soc.* **1965**, 3933−3939.

Table 2. Selected Bond Lengths (Å) and Bond Angles (deg) for $C_{12}F_8B_2(C_6F_5)_2$ (8b)[a]

fragment 1		fragment2	
B1−C1	1.554(2)	B2−C13	1.555(2)
B1−C2A	1.560(2)	B2−C14A	1.558(2)
B1−C7	1.583(2)	B2−C19	1.584(2)
C1−C6	1.389(2)	C13−C18	1.3891(19)
C1−C2	1.4346(19)	C13−C14	1.4374(19)
C2−C3	1.388(2)	C14−C15	1.389(2)
C2−B1A	1.560(2)	C14−B2A	1.558(2)
C3−C4	1.392(2)	C15−C16	1.393(2)
C4−C5	1.365(2)	C16−C17	1.365(2)
C5−C6	1.392(2)	C17−C18	1.392(2)
C7−C12	1.382(2)	C19−C24	1.381(2)
C7−C8	1.386(2)	C19−C20	1.384(2)
C8−C9	1.380(2)	C20−C21	1.379(2)
C9−C10	1.377(3)	C21−C22	1.378(2)
C10−C11	1.382(2)	C22−C23	1.381(2)
C11−C12	1.382(2)	C23−C24	1.384(2)
C1−B1−C2A	119.64(12)	C13−B2−C14A	119.71(12)
C1−B1−C7	120.53(12)	C13−B2−C19	120.67(12)
C2A−B1−C7	119.82(12)	C14A−B2−C19	119.62(12)
C6−C1−C2	117.79(13)	C18−C13−C14	117.69(13)
C6−C1−B1	121.95(13)	C18−C13−B2	122.18(12)
C2−C1−B1	120.24(12)	C14−C13−B2	120.09(12)
C3−C2−C1	117.53(13)	C15−C14−C13	117.43(12)
C3−C2−B1A	122.31(13)	C15−C14−B2A	122.33(13)
C1−C2−B1A	120.12(12)	C13−C14−B2A	120.20(12)

[a] Symmetry transformations used to generate equivalent atoms: (A) $-x, -y + 2, -z$; (B) $-x + 1, -y + 1, -z$.

the smaller angle allowing for greater π communication between the two conjugated systems. This helps to explain why diboraanthracene **8b** is a significantly stronger Lewis acid (vide infra). All bond lengths and angles for **8b** are within normal ranges for fluoroarylboranes,[3a−g,i−m] with the exception of a statistically significant lengthening of the C1−C2 bond distance to 1.435(2) Å, while the other five phenylene C−C bonds have an average bonding distance of 1.384(2) Å. While this expansion may in part be due to withdrawal of π-bonding electron density from the C_6F_4 units by the electron-deficient B centers, note that some C−C elongation at this juncture is also observed in nonfluorinated anthracenes.[23] Furthermore, such C−C bond elongation is seen in other perfluoroarylborane structures with an ortho substitution pattern. The indicated bond lengthening shown in borafluorene structure **6**[3c] (the second

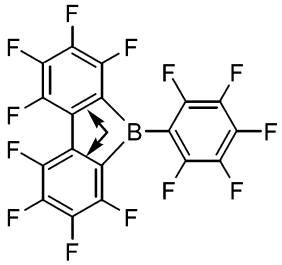

6

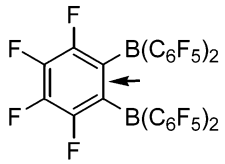

7

bond is symmetry-related) is 1.424(3) Å, significantly longer than 1.382(3) Å, the average phenyl intra-ring C−C bond distance in molecule **6**. Similarly, the indicated bond sketched in structure **7**[3e] has an elongated C−C bond distance of 1.429(2) Å, while the other five

(23) Brock, C. P.; Dunitz, J. D. *Acta Crystallogr., Sect. B: Struct. Sci.* **1990**, *B46*, 795−806.

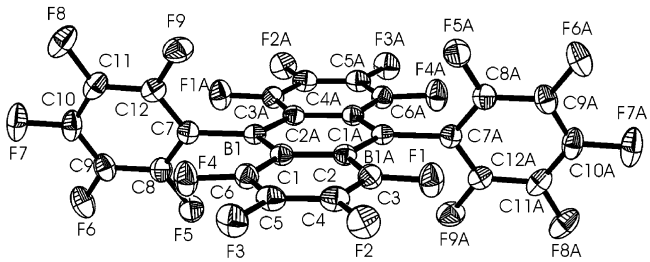

Figure 3. ORTEP diagram of perfluorodiboraanthracene **8b** (50% probability thermal ellipsoids). Important bond distances (Å) and angles (deg) are as follows (distances and angles for only one of the crystallographically independent molecules of **8b** are given; analogous distances/angles for the other molecule are very similar): B1−C1, 1.554(2); C1−C2, 1.435(2); B1−C2A, 1.560(2); B1−C7, 1.583(2); C2−C3, 1.388(2); C3−C4, 1.392(2); C4−C5, 1.365(2); C5−C6, 1.392-(2); C1−C6, 1.389(2); B1−C1−C2A, 120.2(1); C1−B1−C2A, 119.6(2); C1−C2−B1A, 120.1(1); C1−B1−C7, 120.5(1); C2A−B1−C7, 119.8(1).

C−C contacts in the *o*-phenylene ring average 1.382(2) Å.

Lewis Acidic Properties of $C_{12}F_8B_2(C_6F_5)_2$ (8b). To better quantify the Lewis acidity of **8b**, a competition experiment[3g] was carried out in which the strong fluoroarylborane acids **8b** and $B(C_6F_5)_3$ compete for a Lewis base, in this case sterically unencumbered acetonitrile. The relative acetonitrile affinities of **8b** and $B(C_6F_5)_3$ were determined by measuring the equilibrium concentrations of each reactant in eq 3 over a

$$CH_3CN{\rightarrow}\mathbf{8b} + B(C_6F_5)_3 \underset{\text{toluene-}d_8}{\rightleftharpoons} \mathbf{8b} + CH_3CN{\rightarrow}B(C_6F_5)_3 \quad (3)$$

wide temperature range. Concentrations were measured via ^{19}F NMR integration of the $B(C_6F_5)_3$ para ^{19}F signals with and without acetonitrile coordination. The equilibration of **8b** with $CH_3CN{\rightarrow}B(C_6F_5)_3$[3g] over a 77 °C temperature range in toluene-d_8, followed by van't Hoff analysis of the ^{19}F NMR data (Figures 4 and 5), yields $\Delta H = +1.4(2)$ kcal/mol and $\Delta S = -5.3(1)$ eu for eq 3 (Figure 6). These data clearly indicate that **8b** is a stronger Lewis acid than $B(C_6F_5)_3$ with respect to acetonitrile, while $\Delta S < 0$ suggests some loss of degrees of freedom, consistent with greater steric congestion in $CH_3CN{\rightarrow}B(C_6F_5)_3$.

Borafluorene **6**[3c] was designed to exhibit strong Lewis acidity by virtue of a five-membered borole ring having a four-electron, antiaromatic π system. To assess the Lewis acidity characteristics of **6** in a competition experiment analogous to eq 3 (vide supra), the equilibration of acetonitrile between **6** and $B(C_6F_5)_3$, was carried out (eq 4).[3c] It was concluded that at 25 °C in

$$CH_3CN{\rightarrow}B(C_6F_5)_3 + \mathbf{6} \rightleftharpoons CH_3CN{\rightarrow}\mathbf{6} + B(C_6F_5)_3 \quad (4)$$

toluene-d_8 $K_{eq} = 1.30(3)$. In contrast, for **8b** at 25 °C in toluene-d_8, the present work shows that $K_{eq} = 178(1)$. Therefore, perfluorodiboraanthracene **8b** is the strongest boron-based organo-Lewis acid synthesized to date, with the measured ordering of acetonitrile reaction enthalpy (Figure 7) falling in the following progression (kcal/mol): **8b** (−18.5(2)) > **5** (−17.8(2))[3g] > $B(C_6F_5)_3$ (−17.1(9))[3h] > **4** (−11.5(3)).[3h]

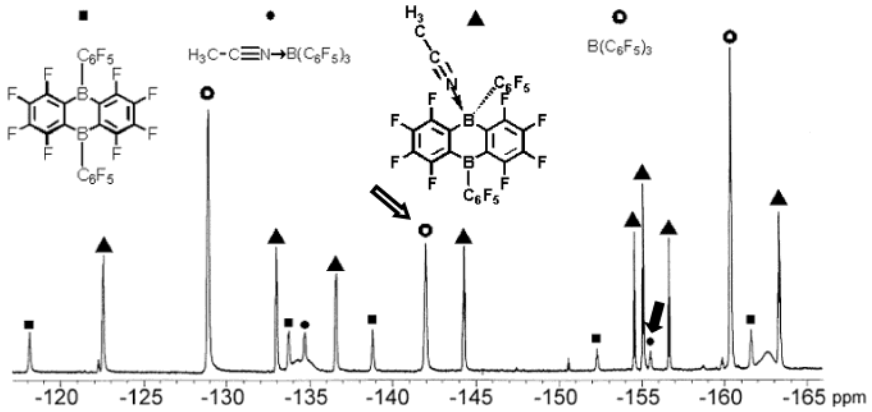

Figure 4. Room-temperature ^{19}F NMR spectrum of acetonitrile equilibration between **8b** and $B(C_6F_5)_3$. The arrows indicate the two peaks that were used to determine the equilibrium constant. The hollow arrow indicates the resonance for the *para* fluorine signal of $B(C_6F_5)_3$, while the filled arrow indicates the resonance for the *para* fluorine nuclei of the acetonitrile adduct of $B(C_6F_5)_3$.

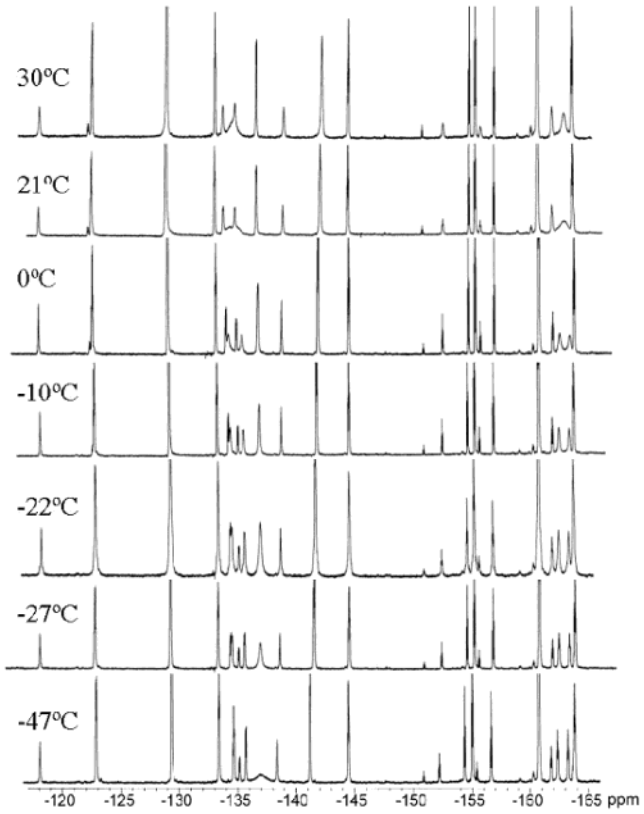

Figure 5. Variable-temperature ^{19}F NMR spectra showing the equilibration of acetonitrile between $B(C_6F_5)_3$ and **8b**. The peaks near δ −134.5 and −162.5 ppm (Figure 4) are observed to broaden and coalesce as the temperature rises, which is attributable to hindered ring rotation of the $-C_6F_5$ ring attached to the boron having a coordinated acetonitrile.

Solid-State Structure of the Acetonitrile Adduct of 8b. The solid-state structure of **8b**←$NCCH_3$ (Figure 8; selected bond distances and bond angles in Table 3) reveals that the $C_{12}F_8B_2$ diboraanthracene core is slightly puckered with an average atomic deviation from the mean plane of 0.094(4) Å (vs 0.013(2) Å in **8b**). The puckering can also be appreciated from the dihedral angle between the C_6F_4 rings, which increases from 0.6(2)° in **8b** to 9.9(3)° in **8b**←$NCCH_3$. The twist angle of the C_6F_5 substituent appended to the trigonal-planar boron, B1, is slightly closer to orthogonality to the B_2C_4 ring in **8b**←$NCCH_3$ (82°) versus that in **8b** (75°). The bond lengths in **8b**←$NCCH_3$ remain generally unchanged from the corresponding parameters in **8b**. However, the bond lengths about atom B8 are lengthened because of the hybridization change to a tetrahedral, four-coordinate environment, with an average B−C(aryl) bond distance of 1.620(4) Å vs 1.575(4) Å for trigonal B1. The bonding distances at the tetrahedral borane center, B8, in **8b**←$NCCH_3$ are rather similar to those in $CH_3CN\rightarrow B(C_6F_5)_3$, where the average B−C(aryl) bond distance is 1.629(4) Å.[24] The bond distances and angles within the acetonitrile fragment of **8b**←$NCCH_3$ (B−N = 1.594(4) Å, C≡N = 1.128(3) Å, ∠B−N≡C = 174.4(3)°, ∠C−C≡N = 178.6(3)°) are also similar to those found in the corresponding acetonitrile adduct of $B(C_6F_5)_3$ (B−N = 1.616(3) Å, C≡N = 1.124(3) Å, ∠B−N≡C 177.1(2)°, ∠C−C≡N 178.9(3)°),[24] except for the slightly shorter B−N distance. The bond distances around uncoordinated boron, B1, in **8b**←$NCCH_3$ remain unchanged from those in **8b**. The C−C skeletal bond elongation in **8b** (C1−C2 = 1.436(2) Å) is more pronounced than in the structure of **8b**←$NCCH_3$, where the analogous bond distances are C2−C7 = 1.421(4) Å and C9−C14 = 1.420(4) Å.

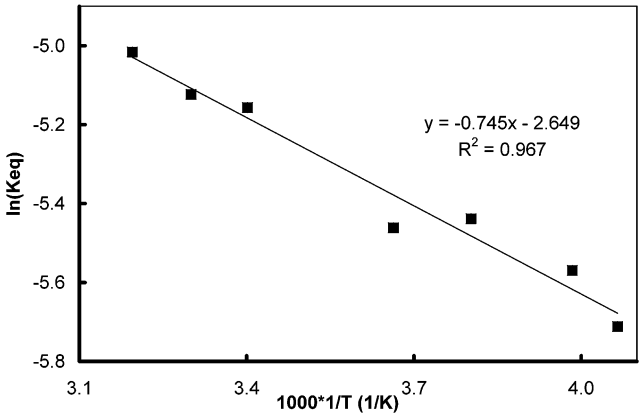

Figure 6. Least-squares van't Hoff plot for the equilibrium $B(C_6F_5)_3$ + **8b**←N $CCH_3 \rightleftarrows CH_3CN\rightarrow B(C_6F_5)_3$ + **8b.**

(24) Jacobsen, H.; Berke, H.; Döring, S.; Kehr, G.; Erker, G.; Fröhlich, R.; Meyer, O. *Organometallics* **1999**, *18*, 1724−1735.

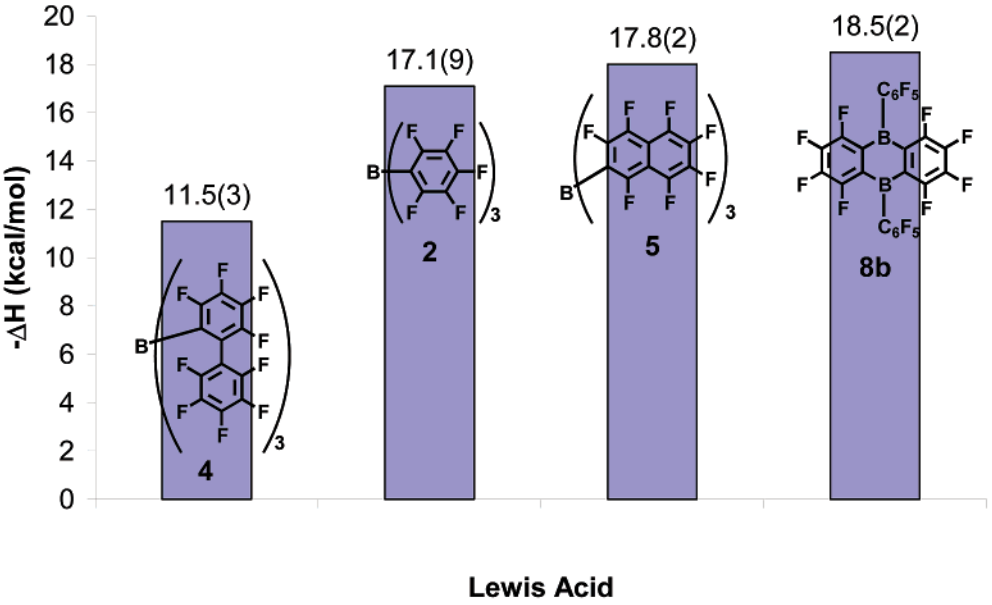

Figure 7. Enthalpies of acetonitrile reaction with the indicated fluoroarylboranes.

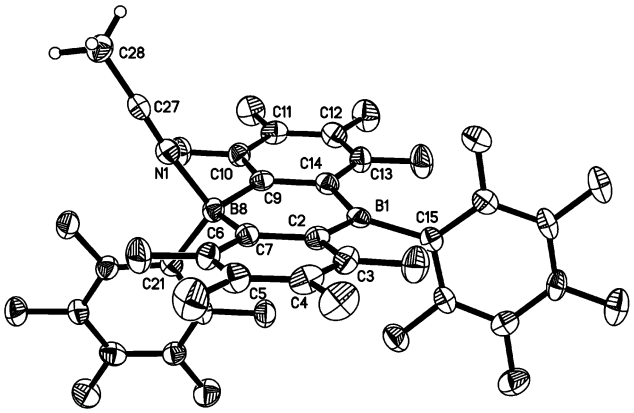

Figure 8. ORTEP diagram of the perfluorodiboraanthracene−acetonitrile adduct **8b**-$NCCH_3$ (50% probability thermal ellipsoids). Important bond distances (Å) and angles (deg) are as follows: B1−C2, 1.548(4); B1−C14, 1.552(4); B1−C15, 1.590(4); B8−C7, 1.608(4); B8−C9, 1.614(4); B8−C21, 1.637(4); B8−N1, 1.594(4); N1−C27, 1.128(3); C2−C7, 1.421(4); C6−C7, 1.383(4); C5−C6, 1.371(4); C4−C5, 1.365(4); C3−C4, 1.380(4); C2−B1−C14, 119.7(3); C2−B1−C15, 119.2(3); C14−B1−C15, 120.8(3); N1−B8−C7, 105.1(2); N1−B8−C9, 105.1(2); N1−B8−C21, 109.5(2); C7−B8−C9, 113.7(2); C7−B8−C21, 112.5(2); C9−B8−C21, 110.4(2); C27−N1−B8, 174.4(3).

Table 3. Selected Bond Lengths (Å) and Bond Angles (deg) for $C_{12}F_8B_2(C_6F_5)_2(NCCH_3)$ (8b-$NCCH_3$)

B1−C2	1.548(4)	B1−C14	1.552(4)
B1−C15	1.590(4)	B8−N1	1.594(4)
B8−C7	1.608(4)	B8−C9	1.614(4)
B8−C21	1.637(4)	N1−C27	1.128(3)
C2−C3	1.396(4)	C2−C7	1.421(4)
C3−C4	1.380(4)	C4−C5	1.365(4)
C5−C6	1.371(4)	C6−C7	1.383(4)
C9−C14	1.420(4)	C10−C11	1.373(4)
C11−C12	1.370(4)	C12−C13	1.369(4)
C13−C14	1.401(4)	C15−C20	1.372(4)
C15−C16	1.387(3)	C16−C17	1.373(4)
C17−C18	1.372(4)	C18−C19	1.374(4)
C19−C20	1.369(4)	C21−C22	1.382(4)
C21−C26	1.387(4)	C22−C23	1.386(4)
C23−C24	1.366(4)	C24−C25	1.364(4)
C25−C26	1.378(4)	C27−C28	1.450(4)
C2−B1−C14	119.7(3)	C2−B1−C15	119.2(3)
C14−B1−C15	120.8(3)	N1−B8−C7	105.1(2)
N1−B8−C9	105.1(2)	C7−B8−C9	113.7(2)
N1−B8−C21	109.5(2)	C7−B8−C21	112.5(2)
C9−B8−C21	110.4(2)	C27−N1−B8	174.4(3)
C3−C2−C7	117.6(3)	C3−C2−B1	122.1(3)
C7−C2−B1	120.2(2)	C4−C3−C2	122.7(3)
C5−C4−C3	119.2(3)	C4−C5−C6	119.3(3)
C5−C6−C7	123.5(3)	C6−C7−C2	117.6(3)
C6−C7−B8	120.1(2)	C2−C7−B8	122.3(2)
C10−C9−C14	117.8(3)	C10−C9−B8	119.5(3)

Cation-Forming Reactivity of $C_{12}F_8B_2(C_6F_5)_2$ (8b) with Metallocene Dimethyls. The reaction of **8b** with complexes such as $(C_5H_5)_2ZrMe_2$ proceeds via clean, quantitative Zr−Me heterolysis to afford catalytically active (vide infra) ion pairs (Scheme 2). The NMR-scale reaction with 1.0 equiv of $(C_5H_5)_2ZrMe_2$ results in complex **10**—the first example of a mixed borane−borate metallocene catalyst. ^1H NMR spectra are typical of an activated zirconocene dimethyl-derived cation, with a $Zr-CH_3^+$ signal at δ 0.66 and a broadened (due to ^{10}B,^{11}B quadrupolar coupling) $B-CH_3^-$ resonance at δ 0.17. All 10 Cp protons are magnetically equivalent with a single resonance at δ 6.34 (indicating a symmetrical structure). The ^{19}F NMR data at 25 °C indicate a static, unsymmetrical structure (5 aryl-F resonances of **8b** become 10 resonances in **10**) with an anionic B−Me^- group and an upfield chemical shift displacement of all ^{19}F resonances (Figure 9). The 25 °C spectrum in CD_2Cl_2 indicates that Zr−Me/B−Me exchange[3i,l] is relatively slow on the NMR time scale under these conditions (no detectable broadening of the Zr−Me resonances), with observable pairs of magnetically nonequivalent B−C_6F_5 ortho and meta ^{19}F signals suggesting restricted B−C_6F_5 rotation.

The reaction of **8b** with 2.0 equiv of $(C_5H_5)_2ZrMe_2$ results in instantaneous formation of a symmetrical bis(metallocenium) adduct having one Cp_2Zr-Me^+ moiety proximate to each B−Me^- center, as evidenced by the four $C_{12}F_8B_2$ core ^{19}F resonances in structure **10** collapsing into two sets of resonances in bis(borate) **11** (Scheme 2; both idealized C_{2v} and C_{2h} structures are in principle possible). This is the first example of a bis-anion paired with two metallocenium cations and

Scheme 2. Reactivity Patterns of Perfluorodiboraanthracene Organo-Lewis Acid 8b with $(C_5H_5)_2ZrMe_2$ in CD_2Cl_2[a]

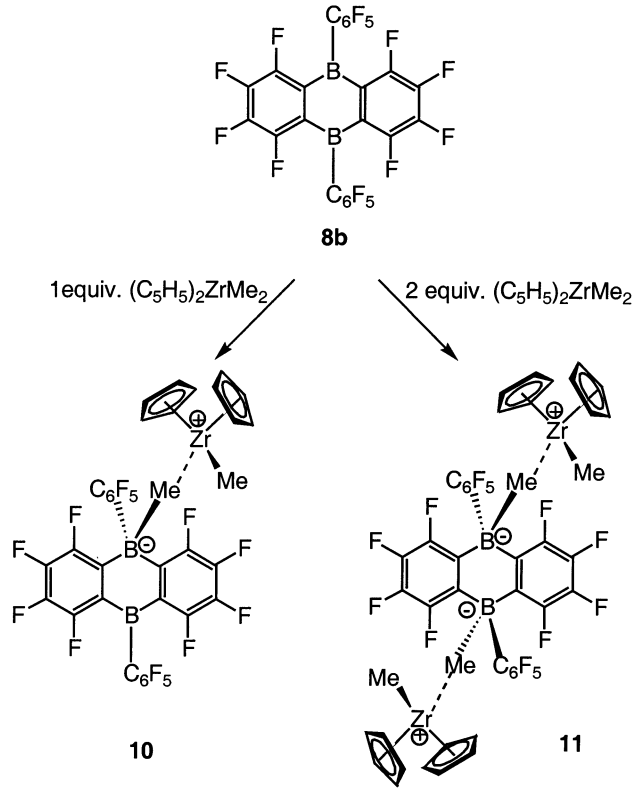

[a] The "trans" isomer of **11** is shown. NMR data do not allow differentiation between cis and trans (idealized C_{2v} vs C_{2h} structure) isomers; however, steric considerations appear to favor the "trans" Cp_2ZrMe^+ disposition.

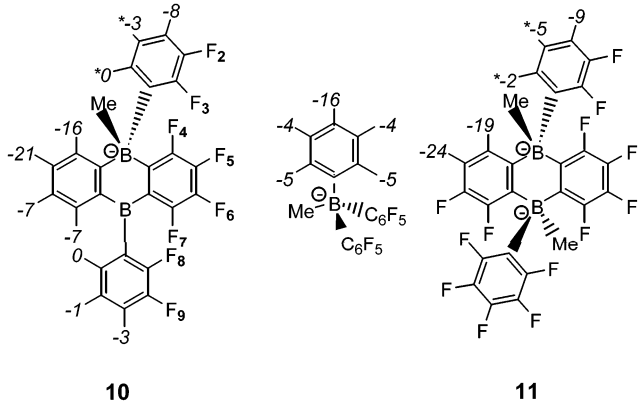

Figure 9. ^{19}F NMR chemical shift displacements for the anions resulting from $B(C_6F_5)_3$ and **8b** after reaction with $(C_5H_5)_2ZrMe_2$. Data are at 25 °C in CD_2Cl_2. Assignments for **10** are based on the assumption that fluoroarylborate ^{19}F signals are displaced further upfield than fluoroarylborane ^{19}F signals. Asterisks indicate chemical shifts that are averaged values for two rotamers.

indicates that *borane−borate **10** is sufficiently acidic to abstract a methide group from a second metallocene dimethyl*. Again, room-temperature ^1H and ^{19}F NMR data indicate an essentially static structure, with slow Zr−Me/B−Me exchange and hindered rotation about the (now magnetically equivalent) $B-C_6F_5$ rings.

The reaction products of diboraanthracene **8b** with 1.0 and 2.0 equiv of $(C_5H_5)_2ZrMe_2$ feature upfield ^{19}F shifts both in the aromatic core and in the appended C_6F_5 substituents (Figure 9). The upfield shifts for the $C_{12}F_8B_2$ core ^{19}F nuclei are significantly greater than those of the C_6F_5 rings, again evidencing minimal π communication between the molecular core and pendant C_6F_5 rings. The upfield shifts of the core ^{19}F nuclei are also much greater than the upfield shifts of the ^{19}F nuclei in $B(C_6F_5)_3$ upon methide abstraction. The larger upfield shifts in the core ^{19}F signals of **8b** are qualitatively consistent with somewhat greater negative charge transfer to the ring system and away from the methide group, resulting in an overall greater dispersion of the negative charge, thus creating a less coordinating anion.

Polymerization Characteristics of 8b-Derived Catalysts. The properties of **8b** as a cocatalyst for homogeneous ethylene and propylene polymerization were characterized and compared to commonly employed cocatalysts using previously described benchtop/vacuum line and large-scale batch reactor methodologies.[3f,g] The complexes $(C_5H_5)_2ZrMe_2$, $(Me_5Cp)_2ZrMe_2$, and $[Me_2Si(Me_4C_5)(^tBuN)]TiMe_2$ (CGCTiMe$_2$) undergo reaction with **8b** to afford extremely active polymerization catalysts (Table 4). In all cases, **8b**-derived polymerization systems yield products having a polydispersity (M_w/M_n) near 2.0, typical of a single-site polymerization catalyst.[1] In general, the **8b**-derived catalysts exhibit significantly higher polymerization activities than the $B(C_6F_5)_3$-based analogues, with relevant comparisons being entries 4 vs 5, 8 vs 9, and 14 vs 15. Activities also appear to be somewhat greater than those of the corresponding $Ph_3C^+B(C_6F_5)_4^-$-activated catalysts (Table 4, entries 2 vs 3 and 4 vs 7, but not 9 vs 11). Note that catalysts from 2.0 equiv of Cp_2ZrMe_2 and 1.0 equiv of **8b**, which presumably contain a *dianionic cocatalyst*, exhibit polymerization activity, polymer molecular weight, and product polydispersity similar to those of the 1:1 analogue (entries 5 vs 6).

The isospecific polymerization of propylene was carried out on the laboratory scale using 1 equiv of **8b** and either 1.0 or 2.0 equiv of *rac*-$Me_2Si(Ind)_2ZrMe_2$ to probe the cooperativity between the two metallocene centers. The 1:1 catalyst system exhibits an activity of 5.7×10^5 g of polymer/((mol of metallocene)(atm of monomer) h), and the resulting polymer has a melting point of 147 °C with an *mmmm* pentad content of 94%. The catalyst system utilizing 2 equiv of metallocene exhibits a slightly lower activity of 4.1×10^5 g of polymer/((mol of metallocene)(atm of monomer) h) and affords a polymeric product with a nearly identical melting point (146 °C) and *mmmm* pentad distribution (93%). These results suggest that there is little cooperative interaction between the two active polymerization sites of an **8b**-derived dianionic cocatalyst ion paired with two metallocenium units.

Entries 9−12 of Table 4 are of special interest because they represent constrained geometry catalyst mediated polymerization runs carried out on a large scale (>200 g of polymer produced in each run), over relatively long polymerization times (15 min), and at relatively high temperatures (70 or 140 °C). Comparing the results between the benchtop/vacuum line and large-scale reactor experiments shows that similar activities are estimated from both procedures. The large-scale polymerizations also demonstrate that the **8b**-derived polymerization catalysts are much more active than the

Table 4. Comparative Olefin Polymerization Results for Group 4 Catalysts Activated by $B(C_6F_5)_3$, $Ph_3C^+B(C_6F_5)_4^-$, and $C_{12}F_8B_2(C_6F_5)_2$ (8b)

entry	catalyst	monomer [a]	amt of cat.,[b] μmol	conditions[c] (°C, s)	polym yield[g]	activity [d,e]	$10^{-3}M_w$[f]	M_w/M_n
1[g]	$(C_5H_5)_2ZrMe^+MeB(C_6F_5)_3^-$	E	15	25, 60	1.0	4.0×10^6	124	2.03
2	$(C_5H_5)_2ZrMe^+Me[C_6F_4B(C_6F_5)]_2^-$	E	7.5	20, 30	0.28	4.5×10^6	218	2.12
3[h]	$(C_5H_5)_2ZrMe^+B(C_6F_5)_4^-$	E	16	25 ,240	11.2	1.08×10^6	2.30	1.64
4[g]	$(C_5Me_5)_2ZrMe^+MeB(C_6F_5)_3^-$	E	15	25 ,60	0.80	3.2×10^6	136	2.54
5	$(C_5Me_5)_2ZrMe^+Me[C_6F_4B(C_6F_5)]^-_2$	E	7.7	20 ,16	0.56	1.6×10^7	135	2.34
6	$[(C_5Me_5)_2ZrMe^+]_2Me_2[C_6F_4B(C_6F_5)]_22^-$	E	16	20, 17	0.92	1.3×10^7	118	2.00
7[h]	$(C_5Me_5)_2ZrMe^+B(C_6F_5)_4^-$	E	16	25, 240	1.3	1.3×10^5	2.63	1.74
8[g]	$Me_2Si(Me_4C_5)(^tBuN)TiMe^+MeB(C_6F_5)_3^-$	E	15	25, 600	0.20	8.0×10^4	1058	9.54
9.	$Me_2Si(Me_4C_5)(^tBuN)TiMe^+Me[C_6F_4B(C_6F_5)]_2^-$	E	10	25, 40	0.04	3.6×10^5		
10.	$Me_2Si(Me_4C_5)(^tBuN)TiMe^+Me[C_6F_4B(C_6F_5)]_2^-$	E	7.9	65, 22	0.50	1.0×10^7	169	2.14
11[i]	$Me_2Si(Me_4C_5)(^tBuN)TiMe^+B(C_6F_5)_4^-$	E	15	25, 60	0.31	1.2×10^6	122	2.70
12[h]	$Me_2Si(Me_4C_5)(^tBuN)TiMe^+MeB(C_6F_5)_3^-$	E/O	2.0	140, 900	131	7.7×10^7		
13[h]	$Me_2Si(Me_4C_5)(^tBuN)TiMe^+Me[C_6F_4B(C_6F_5)]_2^-$	E/O	2.0	140,900	262	1.5×10^8		
14	$Me_2Si(Me_4C_5)(^tBuN)TiMe^+MeB(C_6F_5)_3^-$	P	6.0	70,600	11	1.0×10^5	175	2.10
15	$Me_2Si(Me_4C_5)(^tBuN)TiMe^+Me[C_6F_4B(C_6F_5)]_2^-$	P	0.75	70,600	216	2.0×10^6	182	2.14

[a] E = ethylene, E/O = ethylene + 1-octene, P = propylene. [b] Based on moles of metallocene added. [c] Conditions given: temperature of polymerization and reaction time in sec. [d] Units for entries 1−13: g of polymer/((mol of cationic metallocene) atm h). [e] Units for entries 14 and 15: g of polymer/((g of Ti) h). [f] GPC relative to polystyrene standards. [g] Data from ref 3f. [h] From: Jia, L.; Yang, X.; Stern, C. L.; Marks, T. J. *Organometallics* **1997**, *16*, 842−857. [i] From: Chen, Y.-X.; Marks, T. J. *Organometallics* **1997**, *16*, 3649−3657. [j] For large-scale reactor procedure see Experimental Section.

$B(C_6F_5)_3$-derived systems, with activity ratios similar to those found in the lab-scale polymerizations. NMR analysis of the copolymer microstructures produced in entries 9 and 10 reveals that the 1-octene incorporation level is only marginally higher than in the corresponding $B(C_6F_5)_3$-cocatalyzed processes.

A high degree of Lewis acidity alone does not always guarantee an active catalyst system, as can be seen in Table 4, entry 9. In this case, the least sterically encumbered metal complex, $CGCTiMe_2$, exhibits rather modest activity (10^5 g of polymer/((mol of catalyst) atm h)) when paired with the sterically open cocatalyst **8b** at room temperature. The more open nature of **8b** is also evident in the negative value of ΔS for the formation of $(C_6F_5)_3B{\leftarrow}NCCH_3$ vs **8b**$\leftarrow$$NCCH_3$ (vide supra). Tight-ion pairing in the $CGCTiMe_2$/**8b** catalyst system would presumably lead to a higher activation energy for olefin enchainment. Positive correlations have previously been demonstrated between the "looseness" of catalyst ion pairing and the olefin polymerization rate.[3h,i,5i,6a,25]

Conclusions

Expanding the scope of available perfluoroarylborane frameworks has provided an extremely powerful new organo-Lewis acid that begins to approach the strength of classical inorganic halides in terms of Lewis acidity. The reaction enthalpies of two of the strongest inorganic Lewis acids, BCl_3 and $SbCl_5$, are 4.9 and 1.7 kcal/mol greater, respectively, than that of $B(C_6F_5)_3$ when crotonaldehyde is used as the probe.[3h] This ranking places **8b** approximately on par, in terms of Lewis acidity, with $SbCl_5$. This acidity enhancement is achieved by providing an expansive, electron-deficient molecular framework to disperse anionic charge (for example, large effects are observed on the ^{19}F NMR chemical shifts of the $C_{12}B_2F_8$ core upon methide coordination) and by minimizing conjugative electronic interactions that would transfer electron density from the C_6F_5 substituents to the boron centers (e.g., the imposed twist angles of the C_6F_5 rings lead to poor π electronic communication with the $C_{12}B_2F_8$ core). These results demonstrate the substantial and efficacious differences in organo-Lewis acid characteristics and in those of derived metallocenium ion pairs that can be effected by manipulation of fluoroarylborane cocatalyst architecture. In the present case, highly acidic **8b** abstracts a methide group so effectively that polymerization activity is greatly enhanced when compared to heavily studied and utilized $B(C_6F_5)_3$. Even though **8b** is a very strong Lewis acid, it is apparently not sterically demanding and can lead to relatively low polymerization activity when paired with sterically open precatalysts such as $CGCTiMe_2$. However, when sterically encumbered metallocene dimethyl complexes such as $(C_5Me_5)_2ZrMe_2$ are employed, highly active (10^7 g of polymer/((mol of catalyst) atm h)) polymerization systems are produced. These results support previously proposed positive correlations between cocatalyst Lewis acidity and polymerization activity.[3g,i] Furthermore, cocatalyst **8b** represents the first bifunctional perfluoroarylborane cocatalyst capable of activating 2 equiv of an organo-group 4 dimethyl complex.

Acknowledgment. This research was supported by the U.S. Department of Energy (Contract No. DE-FG 02-86 ER13511). D.J.S. thanks the Dow Chemical Co. for a postdoctoral fellowship. We thank Dr. Mark McAdon and Prof. Eugene Chen for helpful discussions.

Supporting Information Available: Tables giving complete X-ray structural data. This material is available free of charge via the Internet at http://pubs.acs.org.

OM020079B

(25) Deck, P. A.; Marks, T. J. *J. Am. Chem. Soc.* **1995**, *117*, 6128−6129.